

Article

Spray Deposition and Drift as Influenced by Wind Speed and Spray Nozzles from a Remotely Piloted Aerial Application System

Daniel E. Martin ^{1,*}, Jeffrey W. Perine ², Shanique Grant ², Farah Abi-Akar ³, Jerri Lynn Henry ² and Mohamed A. Latheef ¹

¹ United States Department of Agriculture, Aerial Application Technology Research Unit, College Station, TX 77845, USA; mohamed.latheef@usda.gov

² Syngenta Crop Protection, LLC, Greensboro, NC 27409, USA; shanique.grant@syngenta.com (S.G.); jerrilynn.henry@syngenta.com (J.L.H.)

³ Waterborne Environmental Inc., Leesburg, VA 20175, USA

* Correspondence: dan.martin@usda.gov

Abstract: The phenomenal growth of remotely piloted aerial application systems (RPAASs) in recent years has raised questions about their impact on the off-target movement of plant protection products. The spray droplet spectrum is one of the important determining factors that govern droplet trajectories and off-target movement of pesticide particles. A field study was conducted to compare in-swath and downwind spray deposition on ground samplers from a 20 L RPAAS platform, equipped with three different nozzles, which provided fine, medium, and extra-coarse droplet spectra. A fluorescent dye was used as a tracer to determine spray deposition. Airborne spray droplets were measured at 10 and 20 m downwind. Downwind deposition measured on ground samplers showed that the extra-coarse nozzle received significantly fewer deposits than the medium or the fine nozzle. Similarly, the airborne deposition for the extra-coarse nozzle was significantly less compared to either the fine or the medium nozzle. Linear mixed effects modeling confirmed these results and showed that wind speed served as a covariate by refining the deposition differences among nozzles. Results indicated that spray drift from RPAAS platforms may be mitigated by using appropriate nozzles that produce larger droplet spectra. These results will provide aerial applicators with a better understanding of the best management practices to mitigate drift.

Keywords: UAS; UAV; RPAAS; spray drone; deposition; spray drift



Academic Editors: Zhiyan Zhou and Rui Jiang

Received: 29 October 2024

Revised: 8 January 2025

Accepted: 9 January 2025

Published: 16 January 2025

Citation: Martin, D.E.; Perine, J.W.; Grant, S.; Abi-Akar, F.; Henry, J.L.; Latheef, M.A. Spray Deposition and Drift as Influenced by Wind Speed and Spray Nozzles from a Remotely Piloted Aerial Application System. *Drones* **2025**, *9*, 66. <https://doi.org/10.3390/drones9010066>

Copyright: © 2025 by the authors. Licensee MDPI, Basel, Switzerland. This article is an open access article distributed under the terms and conditions of the Creative Commons Attribution (CC BY) license (<https://creativecommons.org/licenses/by/4.0/>).

1. Introduction

Unmanned aerial vehicles (UAVs) or remotely piloted aerial (or aircraft) application systems (RPAASs) have burgeoned recently across the world, transforming traditional farming systems with a novel method of treatment based on autonomous aerial spray technology. Although various market share data for the drone industry have been reported [1], one of the reports projected that the current market is well poised for future expansion, primarily due to government support by various countries, cost efficiency, the introduction of bigger machines to serve sizeable acreage farms, and the integration of precision agriculture and AI technology purported to revolutionize the agricultural sector to provide farmers with efficient land and crop management systems [2]. The market for agriculture drones in the United States was worth USD 1.39 billion in 2021, and growing

at a compound annual rate of 35.79% over the next few years, the spray drone sector is anticipated to reach a total value of USD 11.9 billion by 2028 [3]. With increased production of UAVs, it is expected that the economic benefits to the aerospace industry in the United States will accelerate job growth and the accrual of additional revenue, totaling more than USD 82 billion from 2015 to 2025 [3]. Goldman Sachs reported that the current spray drone technology has already surpassed manned aircraft in endurance, range, safety, and cost efficiency and that the next generation of drones will add greater stealth, sensory, payload, autonomous, and communication capabilities [4].

Concomitant with the phenomenal growth of UAVs in the farming systems in the United States and South Asian countries, there is a growing concern vis-à-vis their adequacy relative to downwind deposition via off-target movement of pest control products. Although the application of pesticides is more regulated in the United States than in many other countries, there is a growing worldwide demand from growers, applicators, and industries to provide supporting data for safely applying pesticides using this newly emerging technology-based spray application system. Accordingly, the OECD and other researchers compiled a comprehensive review of research publications on RPAASs to help support the data requirements necessary for the safe use of this platform [5–7]. In furtherance of the objectives of this team, it is important to generate field-based data to assess and understand the behavior of pest control products when applied by RPAAS platforms and thus contribute real-time data to help develop predictive models describing the fate of spray droplet trajectories when applied by spray drones. Chen et al. [8] studied spray deposition and drift in a field study and found that drift increased with wind speed, while $D_{v0.5}$ droplets decreased, and that $D_{v0.5}$ droplets of 185 μm showed better penetration into rice foliage. Wang et al. [9] studied in-swath deposition and downwind drift of a four-rotor drone equipped with centrifugal nozzles in a field using three different droplet sizes (100, 150, and 200 μm) and under different wind speed conditions. Wang et al. [9] found that when the rotation speed of the centrifugal nozzle increased from 2000 rpm to 17,000 rpm, the DSC classification changed from extra-coarse to fine droplets. In a turf grass ecosystem, Koo et al. [10] found that for the control of crabgrass, the application height should be as low as possible, as total deposition decreased 6% for each meter increase in application height, probably due to evaporation. Wongsuk et al. [11] found that higher flight altitudes and finer droplets resulted in higher drift values, whereas the addition of an adjuvant and the use of an air-induction nozzle reduced drift <3 m aboveground for a six-rotor UAV.

The fate of the spray droplet trajectory when aurally released by manned aircraft was mathematically modeled as early as 1979 to predict the real-time adjustment of flight operations [12]. However, the RPAAS aircraft is more maneuverable than manned aircraft and can safely fly at much lower altitudes with computer-based guidance systems and thus require mathematical tools to make real-time predictions and adjustments of spray deposition under these conditions. Furthermore, RPAASs are commercially available as diverse types with different payload capacities, amounts of motor thrust, and power ratings and are equipped with factory-installed nozzle systems that produce varying spray droplet spectra [13].

Although the spray drift models developed in a wind tunnel help in understanding the fate of spray droplet trajectories in a controlled environment, they do not address spray drift in the field where the vagaries of weather play a dominant but a determinant factor [14]. Realistic benefits expected from this novel technology in farmlands can only be achieved by understanding the fundamental factors that govern efficacious management and operations of RPAASs during each pass of the aircraft.

The objectives of this study were to determine in-swath and downwind deposition of an aerially applied spray solution when released from an RPAAS platform. The spray droplet spectrum has been well documented as an important variable that the aerial applicators utilize to mitigate spray drift. Sprays composed of a larger droplet spectrum tend to move less horizontally or off-target due to greater mass and have reduced time to descend on the crop foliage. For this study, Turbo TeeJet air-induction (TTI) nozzles that produce extra-coarse droplets were compared to extended range (XR) and Turbo TeeJet (TT) nozzles that produced fine-to-medium droplets, respectively.

2. Materials and Methods

This study was conducted in an unpaved area surfaced with gravel in Burleson County, near College Station, TX (30°40' N, 96°18' W). The RPAAS used in this study was a V8A Pro (Homeland Surveillance and Electronics, Casselberry, FL, USA) with a 20 L payload capacity (Figure 1). This study was composed of three treatments, and each treatment was replicated 20 times. In treatment 1, the RPAAS aircraft was equipped with extended range flat-fan spray nozzles, XR 110-01 (Spraying Systems Inc., Wheaton, IL, USA), which provided fine sprays, and treatment 2 consisted of wide-angle flat-fan spray nozzles, TT 110-01 (Spraying Systems Inc., Wheaton, IL, USA), which provided medium sprays, and treatment 3 consisted of extra-coarse sprays provided by air-induction flat-fan spray nozzles, TTI 110-01 (Spraying Systems Inc., Wheaton, IL, USA). The V8A Pro was equipped with four nozzles, two on the right and two on the left side of the boom. The nozzles were 18" (45.7 cm) and 32" (81.3 cm) from the center of the aircraft for inboard and outboard nozzles, respectively (Figure 2).



Figure 1. The V8A Pro aircraft with a 20 L payload capacity, eight (8) rotors, and four (4) spray nozzles on a boom used for this study. The nozzles were 18" (45.7 cm) and 32" (81.3 cm) from the center of the aircraft for inboard and outboard nozzles, respectively.

The aircraft containing a spray mixture of tap water and Vision Pink™ dye (GarrCo Products, Converse, IN, USA) at 20 mL·L⁻¹ was flown perpendicular to the wind ($\pm 30^\circ$) over a 30 m long sampling line (Figure 3). The aircraft was flown at the -2.5 m position at 3 m height and at a ground speed of 3 m·s⁻¹. The spray nozzle pressure was set to 165.5 kPa which was the lowest pressure that could achieve a full flat-fan pattern, which can help reduce drift. However, this low system pressure would result in a lower flow rate (0.46 L/min) which will yield a lower application rate (4.3 to 8.6 L/ha), depending on the spray nozzle. The operational parameters for the V8A Pro aircraft used in this study were in alignment with Martin et al. [15].

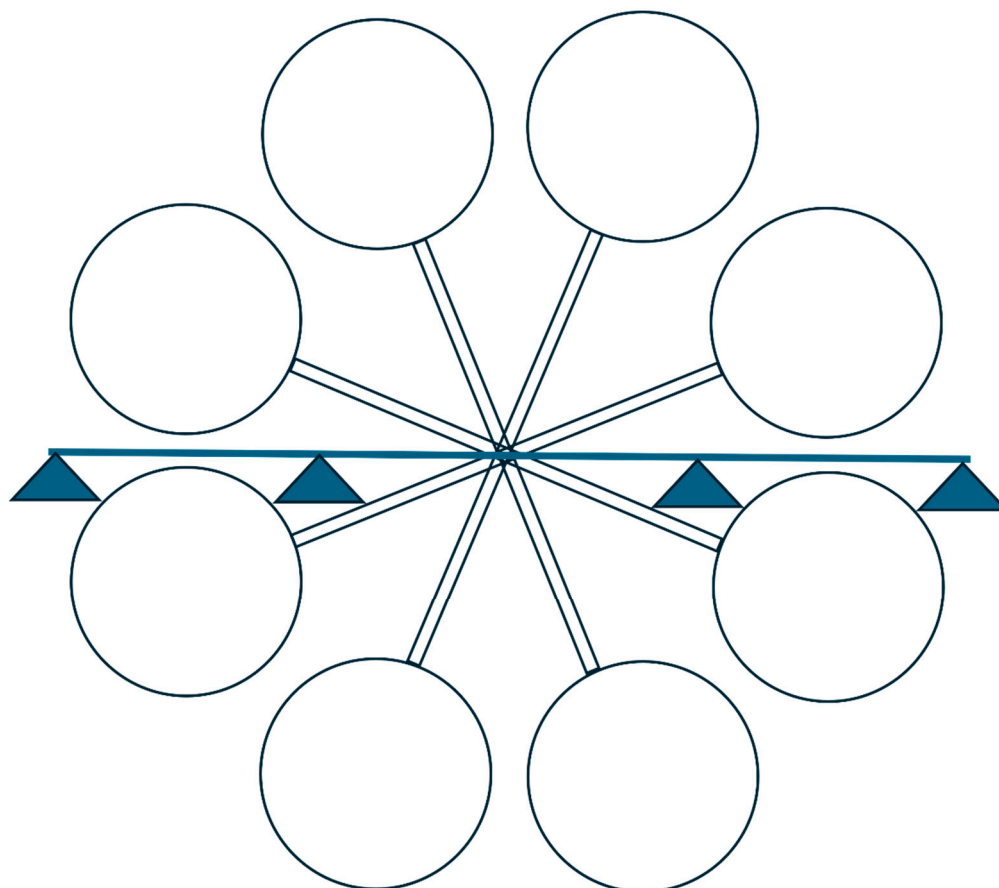


Figure 2. A schematic layout of rotor configurations and nozzle placement on the aircraft boom. Circles represent rotor positions, and the triangles represent the nozzles emitting simulated flat-fan spray patterns. The nozzles were 18'' (45.7 cm) and 32'' (81.3 cm) from the center of the aircraft for the inboard and outboard nozzles, respectively.

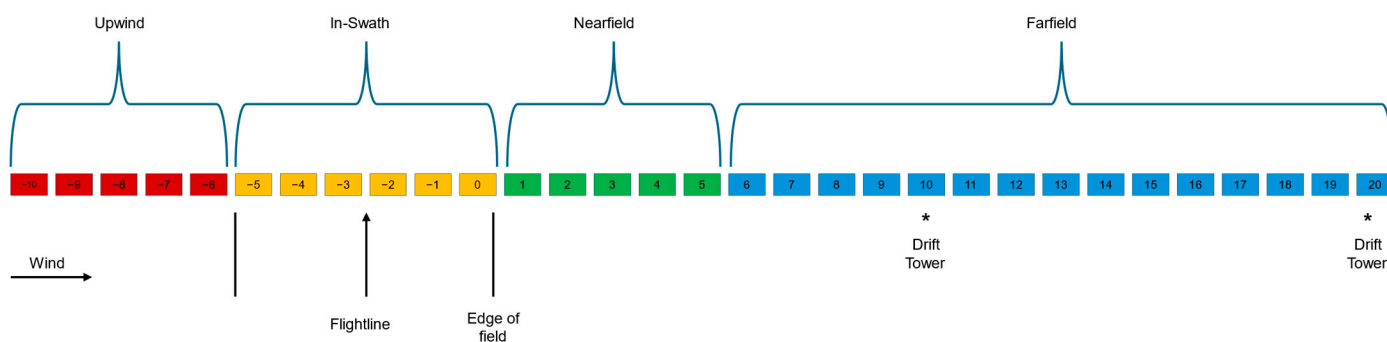


Figure 3. A sampling line where 31 Mylar cards were placed 1 m apart to measure in-swath and downwind deposition. * Drift towers.

The sample line was oriented parallel to the prevailing wind on a caliche surface where ground samplers [Mylar cards (10 cm × 10 cm)] were placed 1 m apart (Figure 3). The sampling line measured in mm was designated as comprising upwind (−10 to −6), in-swath (−5 to 0), near field (1 to 5), and far field positions (6 to 20). The spray droplets were transported parallel to the sampling line where the Mylar cards were placed, perpendicular to the direction of the flight. During each test, spray applications were conducted with a full payload to ensure a maximum, relatively constant, downwash force. The Mylar cards, placed along the downwind edge of the spray swath, as a continuation of the in-swath

samplers, measured the downwind movement, or the drift, of the spray particles. In addition to these samplers, monofilament lines, established parallel with the flight line, were suspended above the ground at 2 m height and at 10 and 20 m downwind of the field edge in each of the three treatments to measure airborne deposition.

Soon after each spray was completed, the Mylar card (100 cm²) and the monofilament samples were placed individually in a plastic bag labeled with the run number, treatment, and replication, stored in an ice chest, and transported to the laboratory for analysis. In the laboratory, 20 mL of ethanol was pipetted into each bag, the bags were agitated forcefully, and 6 mL of the effluent was poured into a cuvette. The cuvettes were then placed into a spectrofluorophotometer (Shimadzu, Model RF5000U, Kyoto, Japan) with an excitation wavelength of 453 nm and an emission at 488 nm. The fluorometric readings were converted to µg of dye/cm². The minimum detection level for the dye and sampling technique was 0.00007 µg/cm².

Prior to the spray drift field tests, the spray droplet spectra for each of these nozzles were determined by flying the V8A Pro aircraft over a sampling line composed of water-sensitive paper (WSP) samplers (76 mm × 26 mm) placed 1 m apart. WSPs were inserted into each of the paper clips mounted on a wooden block before each spray application. The WSPs were removed from the wooden block approximately 1 min after each spray pass was completed and placed inside photonegative sleeves (Model # 35-7BXW; PrintFile[®] Archival Preservers, Apopka, FL, USA). They were then taken to the laboratory for computer-based analysis of the spray droplet images captured on the samplers using the DropletScan[™] scanner-based system [16]. The spray droplet spectra measured were $D_{v0.1}$, $D_{v0.5}$, and $D_{v0.9}$. $D_{v0.1}$ is the droplet diameter (µm) where 10% of the spray volume is contained in droplets smaller than this value. Similarly, $D_{v0.5}$ and $D_{v0.9}$ are droplet diameters where 50 and 90% of the spray volumes are contained in droplets smaller than these values, respectively. The $D_{v0.5}$ is commonly known as the volume median diameter (VMD). The American Society of Agricultural and Biological Engineering (ASABE) has developed a standard to measure and interpret spray quality tips of nozzles used in production agriculture, ASABE S572.3, the Droplet Size Classification [17]. In accordance with this standard, the spray droplet sizes that were released from the spray nozzle tips in this study were composed of fine (106–235 µm), medium (236–340 µm), coarse (341–403 µm), and extra-coarse (404–502 µm) spray droplets.

2.1. Determination of Effective Swath

The effective swath was determined using established methodologies designed for manned aircrafts by the American Society of Agricultural and Biological Engineers (ASABE) [18]. This method is composed of multiple passes (three or more) each lapped one over the other to obtain an average spray pattern, while eliminating passes with deformed or skewed patterns. The aircraft, a V8 Pro equipped with XR 110-01 nozzles, and a fluorescent tracer solution flew into the wind over a 19.2 m long cotton string line in the study area used for the drift tests. The spray passes were replicated 4 times. The cotton string for each pass was analyzed using a fluorometric detection system [19]. Each pass was conducted in a “racetrack” style such that the aircraft flies circuitously and continuously in the same direction. This average spray pattern is then computer-simulated over multiple back-and-forth and racetrack passes. The method used here was consistent with the standard established by Operation S.A.F.E (Self-Regulating Application and Flight Efficiency), sponsored by the National Agricultural Aviation Association, for calibration of fixed-wing and rotary-wing aircraft for spray pattern and drift analysis [20]. The computer simulation will calculate the coefficient of variation (CV) for multiple swath widths. The CV is an index of the uniformity of spray deposit across the swath width and represents the degree of

variation in deposition from the mean [21–24]. An acceptable swath width for the manned aerial applicators is one where the CV $\leq 25\%$. The greater the CV, the more variability there is in the spray pattern. However, Smith et al. [25] reported that a CV of 15% corresponded to a maximum-to-minimum deposit ratio of about 1.7 and indicated that a CV of about 15% or less is a desirable goal for spray applications to minimize overapplication. Figure 4 shows that the effective swath varied from 16 to 26 ft (4.87 to 7.92 m) with acceptable CVs $\leq 15\%$ of variability. For this study, we chose an effective swath of 6 m, because it provided a wider swath where the fine droplets spread across a wider distance.

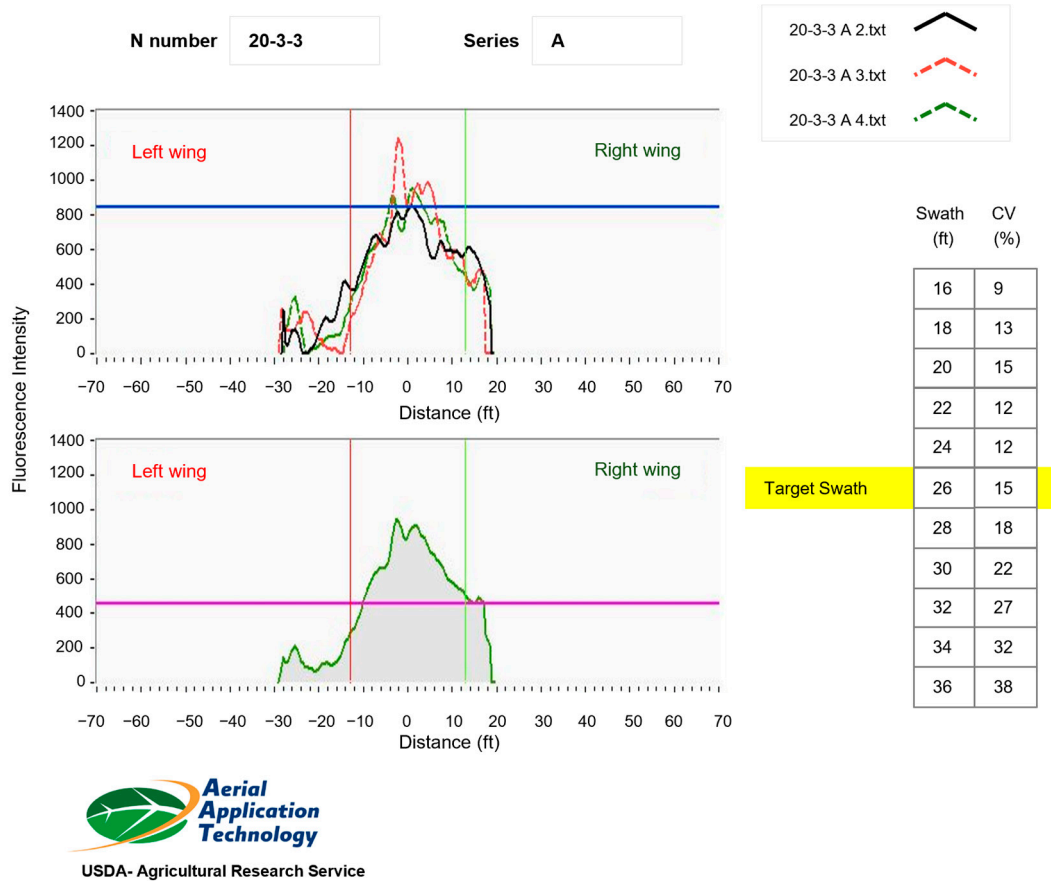


Figure 4. Determination of effective swath for the V8 Pro aircraft equipped with XR 110-01 nozzles. Three passes lapped one over the other provided an effective swath which varied from 16 to 26 ft (4.87 to 7.92 m) with acceptable CVs $\leq 15\%$ (top graph). The average of the three passes is shown in the bottom plot. The blue and purple lines represent the target swath average and combined deposit average, respectively. The vertical lines delineate the 26 ft (7.92 m) target swath width (13 ft or 3.96 m on either side of the center line).

2.2. Meteorological Data

A weather station located at Easterwood Airport, College Station, Texas, was used as the source of wind speed and wind direction data. These data were collected approximately twice every minute. Wind direction was calculated as degrees from parallel to the sampling line, aligned at 143 degrees. Wind speed was measured at a height of 10 m but was converted to 2 m using Equation (1), where V_1 is the measured wind speed at the 10 m height (h_1), V_2 is the estimated wind speed at 2 m (h_2), and Z_0 represents the surface roughness [26,27].

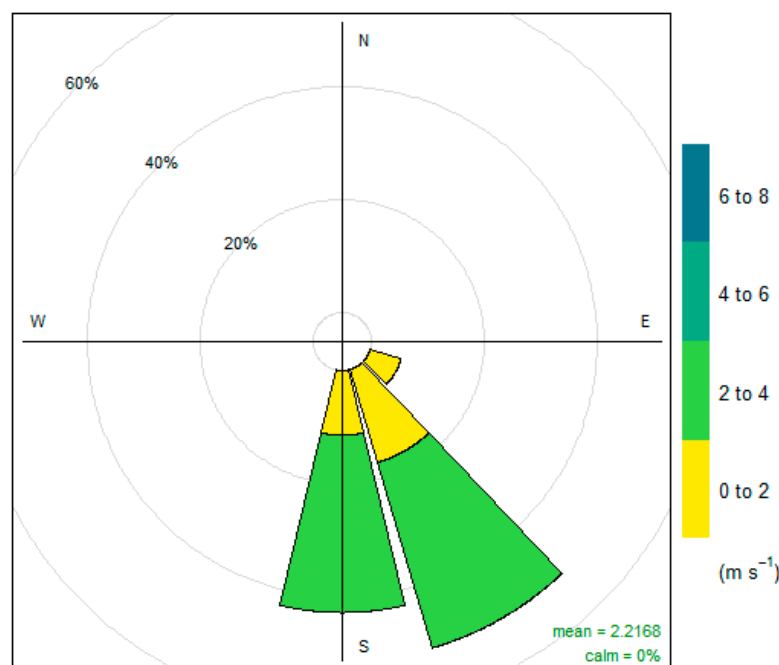
$$V_2 = V_1 \frac{\ln\left(\frac{h_2}{Z_0}\right)}{\ln\left(\frac{h_1}{Z_0}\right)} \tag{1}$$

For this calculation, a surface roughness of 0.03 m was used which represents open agricultural land [27], which accounted for the wind speed being affected by the friction against the surface of the Earth.

The wind measurements were aligned with times for each run as closely as possible, using professional best judgment. If a wind measurement occurred during the spray run time, this single value was used. However, if a wind measurement was not available during the spray run time, measurements flanking the run time were considered. If there were two flanking wind measurements within one minute of the spray run time, the values were averaged. Runs in which the wind direction was $>\pm 30^\circ$ relative to the UAV flight line or that had 0 m/s wind speed were omitted, resulting in 23 runs. This agrees with the ASABE standards S561.1 for determining spray drift by aerial vehicles [28]. Table 1 shows that the meteorological data measured during this study remained stable without any aberrations, and Figure 5 describes the wind direction and wind speed during the tests described in this report.

Table 1. Meteorological data (Mean \pm SEM) measured and calculated for each treatment for this study.

Treatment (Nozzle)	Wind Speed (10 m)	Wind Speed (2 m)	Wind Direction ($^\circ$)	Relative Humidity (%)	Temperature ($^\circ\text{C}$)
Fine	2.08 \pm 0.41	1.51 \pm 0.29	151.5 \pm 7.4	71.3 \pm 2.4	30.8 \pm 0.6
Medium	2.13 \pm 0.38	1.54 \pm 0.28	157.0 \pm 8.4	70.5 \pm 2.4	30.9 \pm 0.6
Extra Coarse	1.87 \pm 0.42	1.35 \pm 0.30	167.8 \pm 9.8	70.0 \pm 2.4	31.1 \pm 0.6



Frequency of counts by wind direction (%)

Figure 5. Wind rose showing the wind speed and predominant wind direction during the field trial.

2.3. Data Analysis

Downwind deposition data on Mylar cards were used to define spray drift curves and to compare between nozzles. Of the 23 runs in which the recorded wind direction fell

in the $<\pm 30^\circ$ range and the wind speed was >0 m/s, there were 9 fine, 8 medium, and 6 extra-coarse nozzle runs each. Drift curves were defined from 1 to 20 m downwind of the drone since the spray swath was assumed to be 6 m wide (3.0 m in either direction). Since all deposition values collected at distances 7.5 m and beyond for the extra-coarse nozzle treatment were $<$ LOD (limit of deposition), they were excluded from this model. The total number of observations used was 424 (14 distances per extra-coarse nozzle run and 20 distances for each of the other nozzles).

Variability in deposition, reported in $\mu\text{g}/\text{cm}^2$, was evaluated using linear mixed-effects (LME) modeling as described by Kuznetsova et al. [29]. To achieve linearity, homoscedasticity, and normality of residuals, deposition was transformed by the cube root and distance was transformed by the natural log. Other fixed-effects variables were the nozzle as a categorical variable, the wind speed in m/s, the cosine of wind angle from parallel, and the combined variable of wind speed \times cosine(angle) to represent both characteristics. The random effects variable was set as a replicate to allow for random intercepts. Statistical analyses were conducted in R software version 4.2.0 [30] including calculation of an R^2_β value [31,32], using the standardized generalized variance approach, and graphs were made with data visualization package, ggplot2 [33].

Differences between in-swath deposition among nozzles were also compared. Deposition collected on Mylar cards at distances from -5 to 0 m, over a 5 m width around the drone's flight line, were summed within replicates. These totals were grouped by nozzle, and an ANOVA test was conducted and a Tukey post hoc test was run to differentiate the nozzles [30]. Residuals were tested to ensure normality and homogeneity of variance.

Besides understanding the effect of spray nozzles on drift, it is equally important to know the differences in deposition between nozzles at each of the sampling locations. Thus, the in-swath and downwind deposition data collected along sampling lines with significant interactions were processed using the least square mean option (adjust = Tukey) of the PROC GLIMMIX procedure [34]. Spray droplet spectra measured before the drift tests were analyzed to determine whether each of the droplet spectrum ($D_{v0.1}$, $D_{v0.5}$, and $D_{v0.9}$) differed between spray nozzles. To make the error variance more nearly constant, the Mylar and the monofilament data were transformed to $X + 1$ and Normal Quantile transformations, respectively, before performing ANOVA. Graphical illustrations of the data were conducted using the SAS/JMP[®] [35] software using the untransformed data.

3. Results

3.1. Droplet Size Classification

Spray plumes exiting the nozzles were composed of fine, medium, and extra-coarse droplets. ANOVA analysis showed that all droplet spectra varied significantly between the nozzles tested ($D_{v0.1}$: $F = 16.68$; $p < 0.0001$; $D_{v0.5}$: $F = 18.22$; $p < 0.0001$; and $D_{v0.9}$: $F = 8.68$; $p < 0.0006$) with MSE df = 46 for all droplet spectra. Figure 6 shows that the $D_{v0.1}$ droplets were significantly smaller for fine and medium nozzles than those for the extra-coarse nozzles. The $D_{v0.1}$ droplets were comparable between fine and medium nozzles. Similarly, the $D_{v0.5}$ droplets were smaller for the fine and the medium nozzles than those for the extra-coarse nozzle. The $D_{v0.9}$ droplets were significantly larger for the medium and the extra-coarse nozzles than those for the fine nozzle. The $D_{v0.9}$ droplets for the medium and the extra-coarse nozzles were comparable.

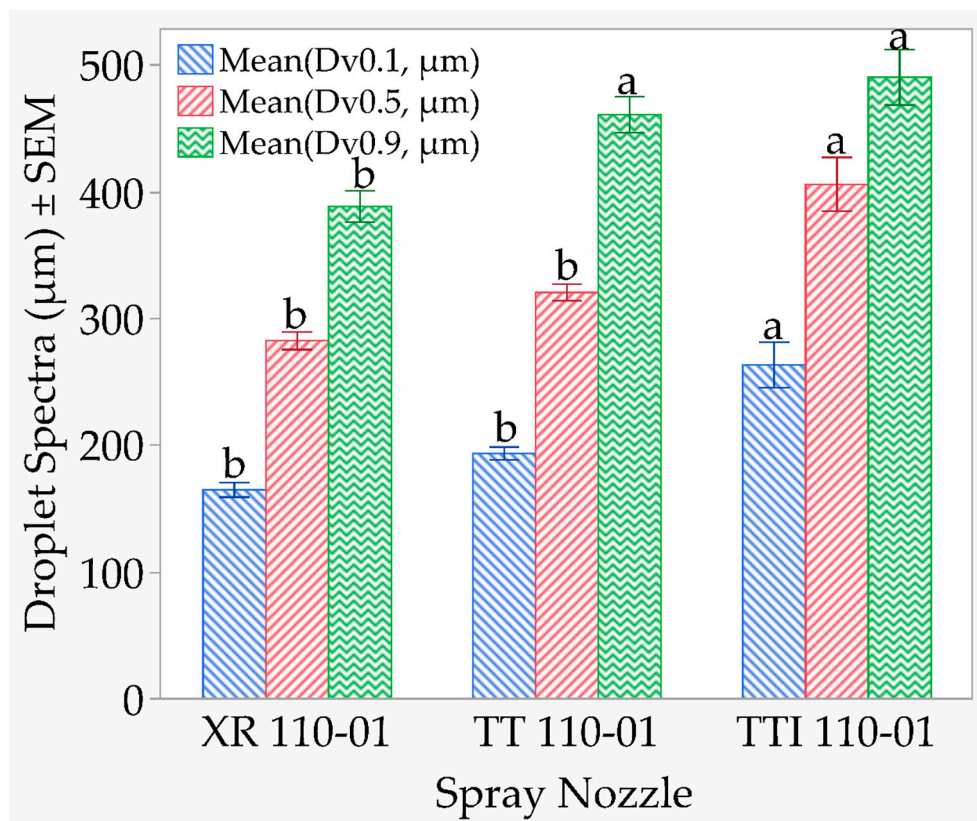


Figure 6. Spray droplet spectra of the spray nozzles (fine, medium, and extra coarse) used in this study. The droplet images captured on WSP samplers were analyzed using computer-based software. Means \pm Standard Error of the Mean (SEM) between spray nozzles within each droplet spectrum followed by the same lower-case letters are not significantly different at $\alpha = 0.05$ (Tukey's HSD test).

3.2. Deposition on Mylar Cards

The variance analysis of upwind, in-swath, and near-field deposition on Mylar cards showed a significant interaction with sampling locations ($F = 2.63$; $df = 30, 320$). Figure 7 shows that beginning at the upwind location of -6 m, significantly fewer deposits occurred for the extra-coarse nozzle, but differences were not significant between extra-coarse and fine nozzles. However, deposition for the extra-coarse nozzle was significantly less than that for the medium nozzle. A similar trend persisted at the -5 m in-swath location. Deposition in the in-swath region increased for the extra-coarse nozzle until the location at -3 m when significantly more deposits occurred for the extra-coarse nozzle compared to either the medium or the fine nozzle. Increased deposition for the extra-coarse nozzle at the in-swath locations persisted until -1 m when the trend was reversed with deposition for the extra-coarse nozzle declining significantly and asymptotically. The near field deposition was significantly lower for the extra-coarse nozzle than that for either the medium or the fine nozzle.

Figure 8 shows the downwind transport, or the drift, of the applied solution released from the aircraft. Significant differences between treatments were evident from position 6 to 17 m when the deposition for the extra-coarse nozzle was significantly less compared to the fine nozzle. The deposition for the extra-coarse nozzle was significantly less than the medium and the fine nozzle from position 6 to 8 m downwind, but there was no significant difference between the fine and medium nozzles. However, significant separation in deposition between all three nozzles was evident from the 9 to 12 m positions downwind. The extra-coarse nozzle continued to receive significantly less deposition than the fine nozzle from position 13 to 17 m downwind. No significant difference between nozzles were detected thereafter.

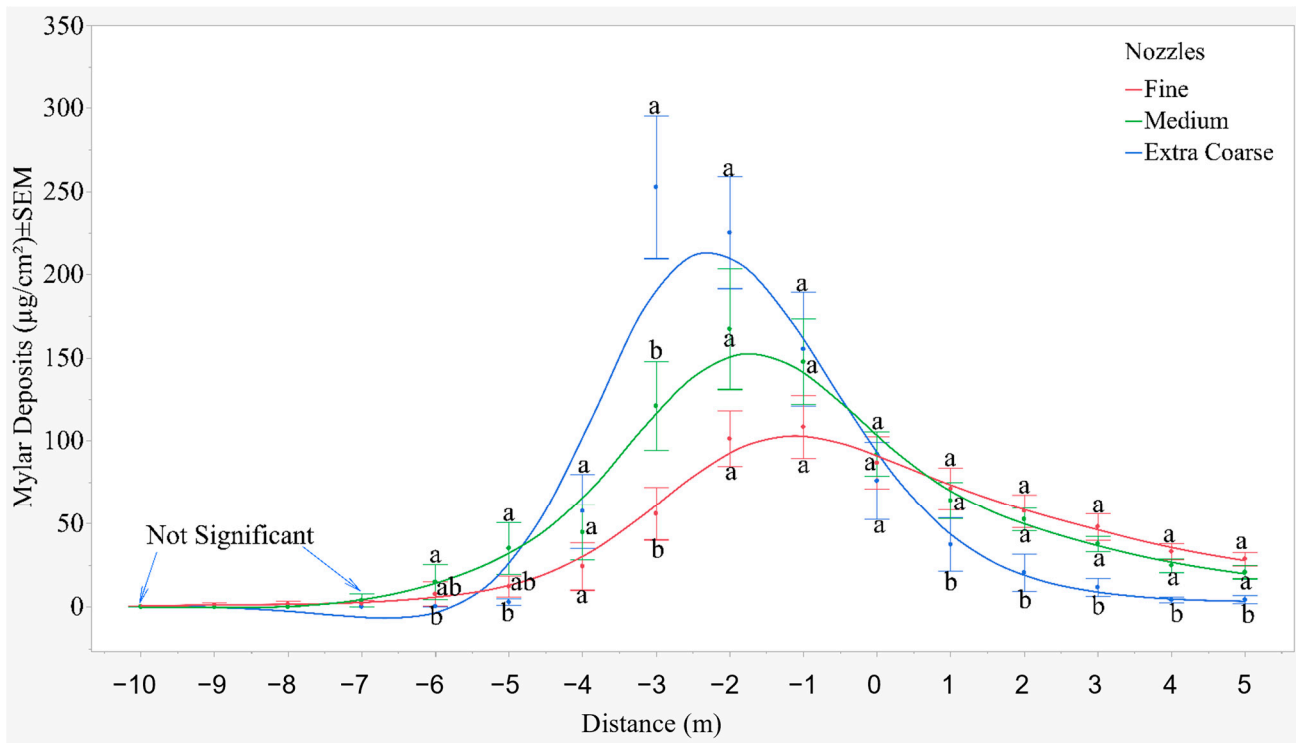


Figure 7. Spray deposition on Mylar cards. Data were analyzed using $\log x + 1$ transformation, but original means are presented here. Means \pm Standard Error of the Mean (SEM) within each sampling line location with the same lower-case letters are not significantly different at $\alpha = 0.05$ (Tukey’s HSD test).

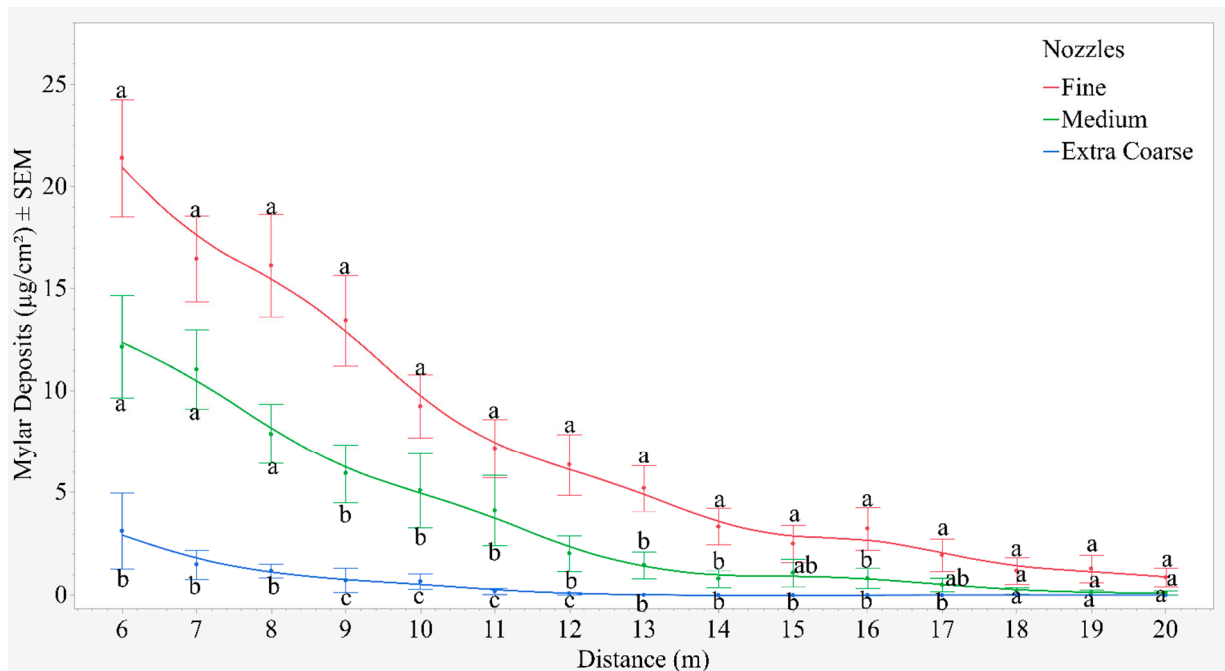


Figure 8. Downwind spray deposition on Mylar cards. Data were analyzed using $\log x + 1$ transformation, but original means are presented here. Means \pm Standard Error of the Mean (SEM) within each sampling line location followed by the same lower-case letters are not significantly different at $\alpha = 0.05$ (Tukey’s HSD test).

3.3. Downwind Spray Deposition Curves

Variability in spray drift deposition downwind of the drone was defined using LME modeling. Details of the model are shown in Table A1 (Appendix A), and the residuals are shown in Figure 9. The R^2_β value was 92% overall, and residuals appeared linearly and normally distributed. The model is summarized with the following formula, which can be used to estimate average deposition at different distances, wind speeds, and nozzles (Equation (2)).

$$\text{Deposition} = (4.94 - 1.28\ln(\text{Dist}) + 0.82W - 0.36N_M - 1.31N_C - 0.30[\ln(\text{Dist}) \times W])^3 \quad (2)$$

where deposition is in $\mu\text{g}/\text{cm}^2$; Dist = distance in m; W = wind speed in m/s; N_M = a binary indicator of the medium nozzle (1 where the nozzle is medium; 0 where it is not); and N_C = a binary indicator of the extra-coarse nozzle. The fine nozzle is the base model and is therefore predictable by setting the N_M and N_C variables equal to zero.

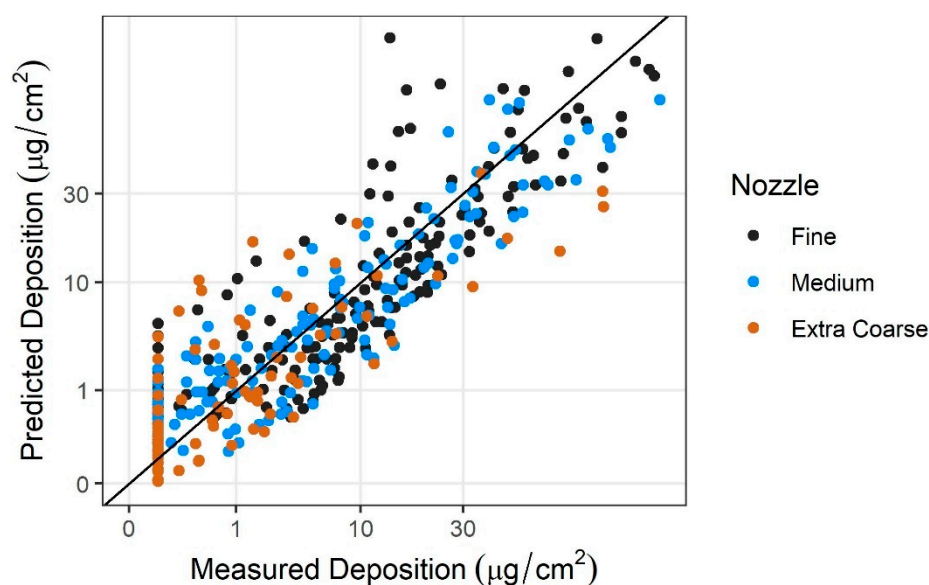


Figure 9. Graph of residual errors from the downwind spray drift deposition LME model. Points above the 1:1 line were overestimated, and those below were underestimated. Predictions were calculated without random effect shifts. Both axes are graphed on the cube root scale, as modeled.

The extra-coarse nozzle produced significantly reduced deposition compared to both of the other nozzles ($p = 0.0018$ versus medium, and $p = 0.0001$ versus fine, calculated using the package emmeans [36]). For example, at the closest distance downwind of 3.5 m from the drone and at the mean wind speed (2.1 m/s), extra-coarse-nozzle runs produced $34.0 \mu\text{g}/\text{cm}^2$ less than medium-nozzle runs on average, and $52.8 \mu\text{g}/\text{cm}^2$ less than fine-nozzle runs on average. However, 20.5 m from the drone, extra coarse < medium by only $0.2 \mu\text{g}/\text{cm}^2$ on average and extra coarse < fine by $0.8 \mu\text{g}/\text{cm}^2$ on average.

Though the nozzle variable overall was significant ($p = 0.0005$), the medium nozzle's deposition was like that of the fine nozzle ($p = 0.14$). These two nozzles' sets of replicates had wide variability, with enough overlap to result in confidence intervals too wide to differentiate the two nozzles (see overlap in shaded 95% confidence intervals in Figure 10).

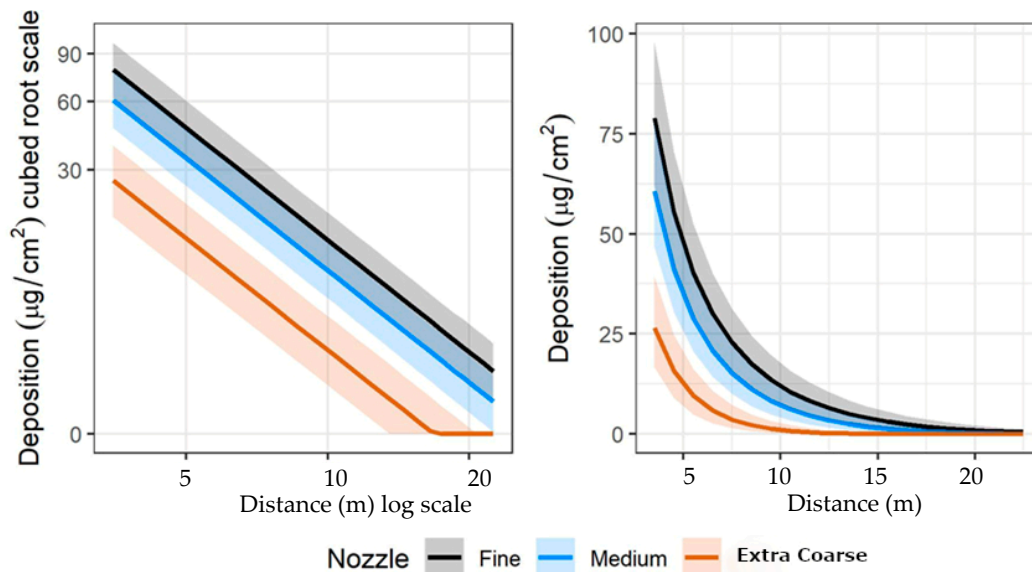


Figure 10. Downwind spray drift deposition curves for each nozzle with shaded 95% confidence intervals, shown at the mean wind speed (2.1 m/s). **(Left):** axes scaled as modeled; **(Right):** standard scale. The fine and medium nozzles are more similar in range compared to the distinctly lower extra-coarse nozzle. From 7.5 m and on, extra-coarse nozzle depositions were predicted as nondetectable.

Faster wind speed was associated with greater deposition at distances close to the drone (p value of intercept shift = 0.0004), with differences indistinguishable at farther distances (p value of slope shift < 0.0001). This attenuation of wind speed effect is visible in Figure 11. Wind speed correlated with and partially explained variability in the deposition. Wind speed, therefore, served as a covariate by refining the mean differences among nozzles.

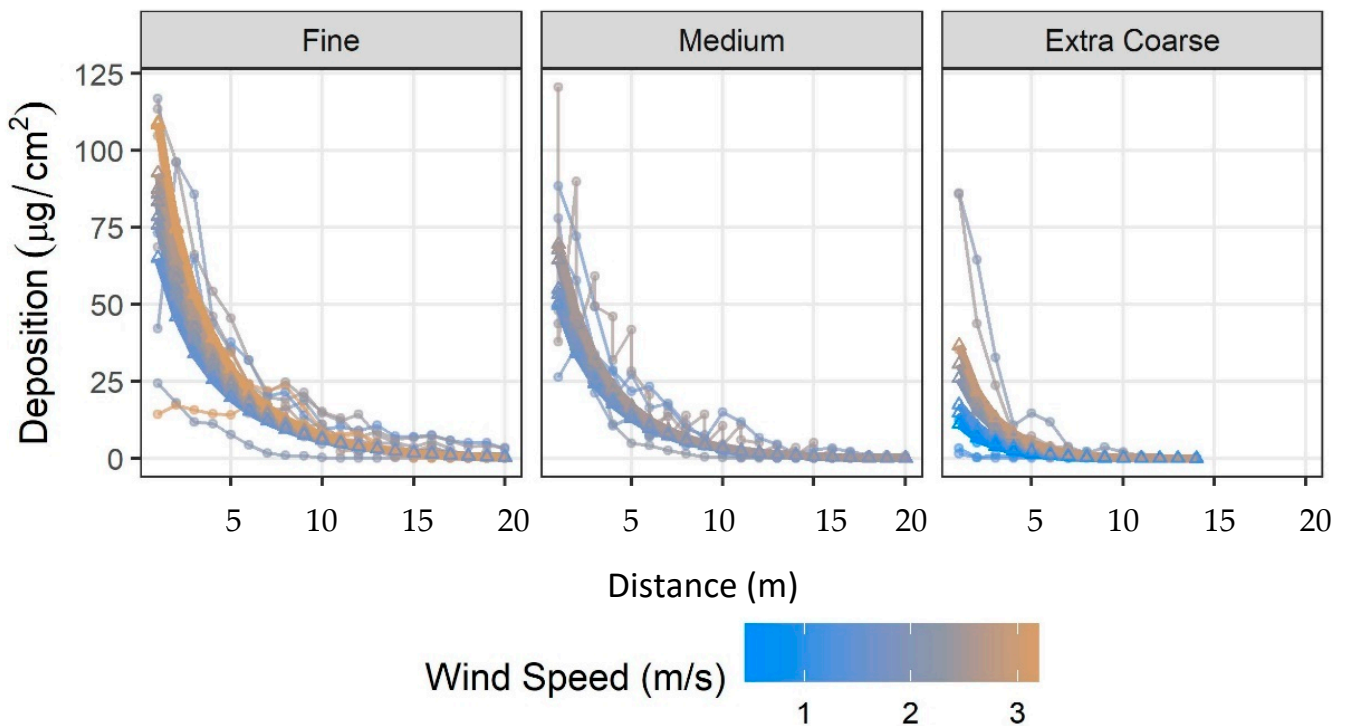


Figure 11. Actual downwind depositions (thinner lines with circle points) and predicted depositions from the LME model (thicker lines with triangles). Wind speed varied the predictions, such that faster speeds had greater depositions at closer distances.

Of note, one point was not well-predicted in this model. During fine nozzle replicate 7, the closest downwind distance of 3.5 m was measured to be $14.3 \mu\text{g}/\text{cm}^2$ but was predicted as $109.0 \mu\text{g}/\text{cm}^2$. The shape of this run's deposition curve was unique in that values from distances 3.5 to 9.5 were nearly flat, rather than decreasing as would be expected. This run had the maximum wind speed among the runs used in this analysis (3.2 m/s), but otherwise, no data existed to explain its uniqueness.

3.4. Deposition on Monofilament Lines

The deposition on monofilament lines as the driftable component of the spray application is shown in Figure 12. The variance analysis indicates that the spray nozzle ($F = 29.78$; $p < 0.0001$; $df = 2, 113$) and the location of the samplers as sources of variation were highly significant ($F = 22.89$; $p < 0.01$; $df = 1, 113$) with no significant interaction between them ($F = 2.70$; $p > 0.007$; $df = 2, 113$). Deposition decreased significantly as sampling distance downwind increased. The extra-coarse nozzle produced less airborne deposition compared to either the fine or the medium nozzle at both the 10 and 20 m sampling distance. The fine nozzle predominated with higher airborne deposition at the 10 m distance downwind. A similar trend in deposition was observed at the 20 m distance downwind as well for the fine nozzle, but it was comparable to that for the medium nozzle. Overall, deposition on monofilament lines averaged 14.80 ± 1.77 , 5.51 ± 1.16 , and $0.37 \pm 0.12 \mu\text{g}/\text{cm}^2$ for fine, medium, and extra-coarse nozzles, respectively, and these values were significantly different from one another (Figure 13).

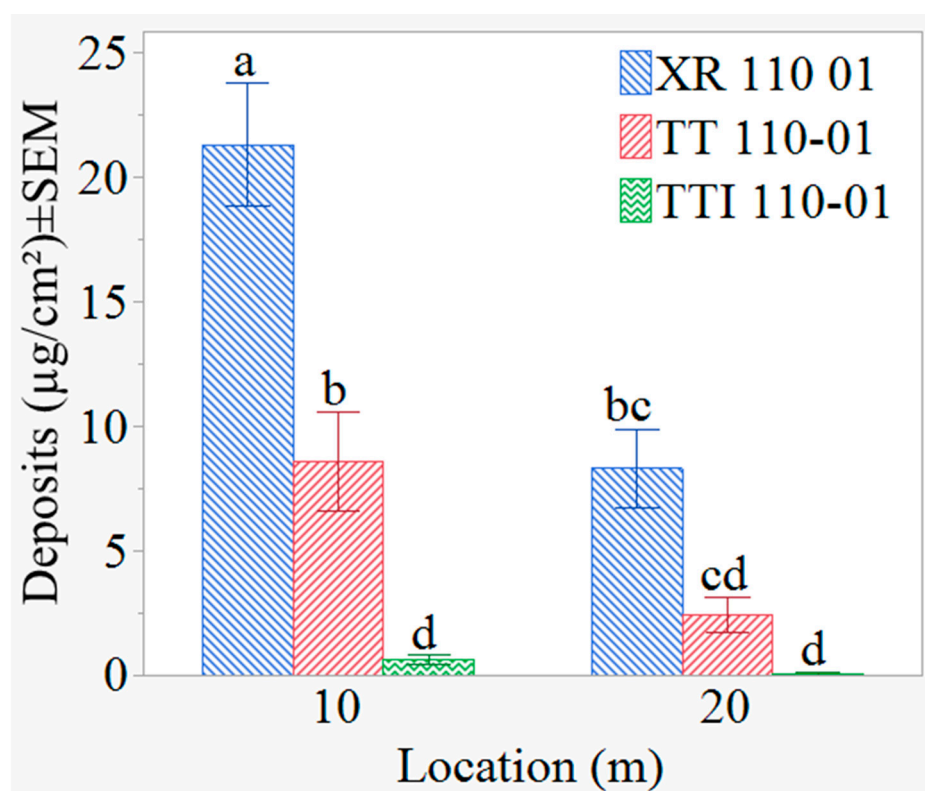


Figure 12. Deposition on monofilament lines at 10 and 20 m distance downwind. Means \pm Standard Error of the Mean (SEM) with the same lower-case letters are not significantly different at $\alpha = 0.05$ (Tukey's HSD test). The data were analyzed using the Normal Quantile transformation, but the results are presented as original means.

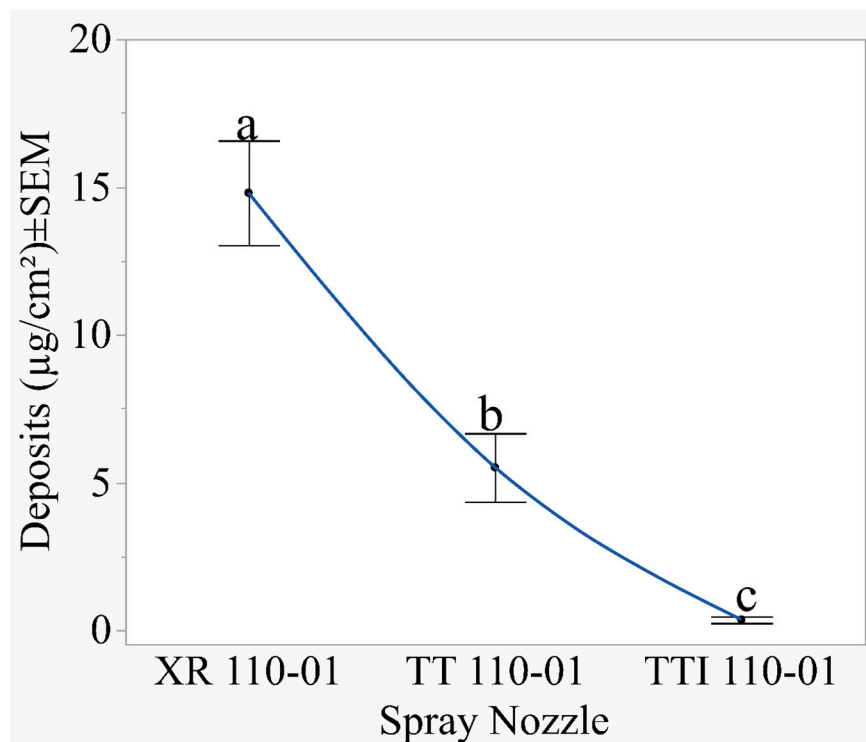


Figure 13. Overall spray deposits on monofilament lines established for the fine, medium, and extra-coarse nozzle treatments. Means \pm Standard Error of the Mean (SEM) followed by the same lower-case letters are not significantly different (HSD test) at $p = 0.05$. The data were analyzed using the Normal Quantile transformation, but the results are presented as original means.

4. Discussion

Researchers have reported that fine spray droplets were often the primary cause of agrochemical spray drift, while extra-coarse droplets produced by air-induction nozzles were less prone to drift. This study shows that as the droplet size increased, the spray drift or the movement of spray particles downwind decreased. The TTI 110-01, a flat-fan air-induction nozzle (extra-coarse droplets), produced the lowest spray deposition on Mylar cards downwind of the swath. This is in alignment with Wang et al. [37] who studied spray drift potential for UAVs in a controlled wind tunnel and found the air-induction nozzle produced less drift compared to hollow-cone or flat-fan nozzles. Data in this study also showed that deposition on the monofilament lines from the drift towers established at two different distances downwind was significantly less for the air-induction nozzle compared to fine and medium nozzle treatments. The importance of droplet size and, therefore, the spray nozzles are important factors for characterizing spray drift. Smaller and fine highly driftable droplets move downwind, while the drift-prone extra-coarse droplets fall under the fuselage of the aircraft. Coarse spray droplets have greater mass and sustain a downward velocity in the air for a longer time than fine droplets before they descend to the target sites and thus cause less drift.

This study demonstrates that wind speed is an essential covariate influencing the trajectory of spray droplets. Notably, the lowest wind speeds occurred during the test when the drone was equipped with an extra-coarse nozzle. To evaluate the potential impact of this coincidence on downwind spray drift, we reran the LME model excluding these two instances. The analysis revealed that the intercept of the wind speed variable was not significant ($p = 0.113$), although the negative slope remained significant ($p = 0.026$), indicating that wind speed's explanatory power was reduced, but its directional influence persisted. Additionally, removing these data points slightly increased the estimate for the extra-coarse nozzle (coefficient changed from -1.31 to -1.27), yet it remained statistically

significant, confirming that the results were not substantially affected by these specific conditions. These findings from the LME model highlight the benefit of using modeling to assess the impact of covariates such as wind speed on spray drift. This method provides a foundational platform for enhancing our understanding and prediction of drift behavior under various conditions and is complementary to field research.

Teske et al. [38] reported that the rotor downwash of UAVs could facilitate the movement of spray materials to the ground under critical application speed. At a lower flight speed, the strong downwash beneath the rotors is likely to push the sprays to the ground more quickly and improve spray distribution on target sites. However, under higher application speeds, the turbulence created could reduce the downwash force and help in the off-target movement of spray materials. In this study conducted under optimal ground speed, it appears that the RPAAS propellers could have helped the spray solution to reach the target and thus achieve the intended objectives of this study. Hunter et al. [39] reported that the wind currents at a higher application height may carry driftable particles farther than the intended area compared to the application height used in this study.

Using a modeling approach, Yang et al. [40] reported that the distance spray droplets can travel upon exiting the nozzle are controlled by horizontal and vertical forces from a UAV aircraft. Teske et al. [38] reported that it is important to identify the ground speed of a UAV when the downwash from the rotors becomes outwash before the spray materials reach the target site. At an increased ground speed, the interaction between perpendicular wind conditions is likely to increase off-target transport of spray products. Atmospheric stability and wind conditions are more likely factors that impinge upon the off-target movement of spray droplets.

One of the limitations of this study was that the wind speed measurements in time were used from a nearby weather station. Thus, there is uncertainty associated with the wind speed data associated with each run. Since wind speed and wind direction varied frequently from one minute to the next, it is likely that at least some of the runs associated with wind speed measurements did not represent actual wind conditions onsite. A greater reliance on model predictions of field data would require more robust and on-site measurements of weather conditions.

5. Conclusions

With the phenomenal growth of remotely piloted aerial application systems in production agriculture in recent years, there is a growing demand from applicators of aerial application systems to provide them with guidelines for applying pest control products with minimum spray drift. It is well documented that spray nozzles play a dominant role in the downwind deposition of driftable spray particles. Accordingly, this study sought to assess the effects of three different nozzles with fine, medium, and extra-coarse spray droplet spectra on in-swath and downwind deposition. Monofilament lines to measure airborne drift were established out to 20 m downwind from the edge of the field. The spray droplet sizes that were released from the spray nozzle tips in this study were composed of fine (106–235 μm), medium (236–340 μm), coarse (341–403 μm), and extra-coarse (404–502 μm) spray droplets. Results indicated that the extra-coarse nozzle was associated with reduced downwind and airborne deposition compared to both medium and fine nozzles. Wind speed served as a covariate in refining the differences in deposition between nozzles. Results also suggested that smaller, fine, and highly driftable spray droplets move downwind while extra-coarse and very large droplets tended to fall directly under the fuselage of the aircraft. Remote pilots of aerial application systems may adopt this technology as a best management practice to mitigate spray drift.

Author Contributions: Conceptualization, D.E.M. and J.W.P.; Data curation, D.E.M., J.W.P., F.A.-A. and M.A.L.; Formal analysis, D.E.M., J.W.P., F.A.-A., J.L.H. and M.A.L.; Funding acquisition, D.E.M. and J.W.P.; Investigation, D.E.M. and J.W.P.; Methodology, D.E.M. and J.W.P.; Project administration, D.E.M. and J.W.P.; Resources, D.E.M. and J.W.P.; Software, D.E.M.; Supervision, D.E.M.; Visualization, D.E.M.; Writing—original draft, D.E.M., J.W.P., F.A.-A. and M.A.L.; Writing—review and editing, D.E.M., J.W.P., S.G. and M.A.L. All authors have read and agreed to the published version of the manuscript.

Funding: This research was funded by Syngenta Crop Protection LLC, grant number 58-3091-9-015.

Data Availability Statement: Data available upon request.

Acknowledgments: The authors would like to thank Richard Crosby with Coastal Sprays for providing and piloting the RPAAS. In addition, the authors would like to thank Cory Southam with Hawks Agro and Gray Turnage and Logan Renz from Mississippi State University for their valuable assistance in conducting the field study.

Conflicts of Interest: During the study period, Jeffery W. Perine, Shanique Grant, and Jerri Lynn Henry were employees of Syngenta Crop Protection, LLC, and Farah Abi-Akar was an employee of Waterborne Environmental, Inc. This study received funding from Syngenta Crop Protection, LLC. The authors declare no additional conflicts of interest beyond these employment relationships and roles in the study. The authors declare that the research was conducted in the absence of any commercial or financial relationships that could be construed as a potential conflict of interest. The use of trade, firm, or corporation names in this publication is for the information and convenience of the reader. Such use does not constitute an official endorsement or approval by the United States Department of Agriculture or the Agricultural Research Service of any product or service to the exclusion of others that may be suitable.

Appendix A

Table A1. LME model results describing variability in downwind spray drift deposition. Significance level of 0.05 (p -value $< 0.05 = *$ (significant); ns = not significant).

Random effects:					
Groups	Standard Deviation	Number of Groups			
Replicate	0.4598	23			
Residual	0.3806				
Fixed effects:					
Variable Explaining $\sqrt[3]{\text{Deposition in } \mu\text{g}/\text{cm}^2}$	Coefficient	Standard Error	Degrees of Freedom	p Value	
Intercept	4.9403	0.5274	42.7	6.54×10^{-12}	*
ln (Distance)	-1.2805	0.1323	400.3	$<2.0 \times 10^{-16}$	*
Wind speed	0.8204	0.2148	52.6	0.000356	*
Nozzle: medium	-0.3596	0.2346	18.9	0.141789	ns
Nozzle: Extra coarse	-1.3076	0.2766	19.2	0.000142	*
ln (Distance) \times Wind speed	-0.2953	0.059	400.3	8.39×10^{-7}	*

References

- Zanelli, E.B.; Bödecker, H. Drone Market Report 2023–2030; Drone Industry Insights. 2023. Available online: <https://dronelli.com/product/drone-market-report> (accessed on 4 June 2024).
- Howe, S. What’s Driving Growth in the Crop Spraying Drone Market? Available online: <https://www.commercialuavnews.com/europe/what-s-driving-growth-in-the-crop-spraying-drone-market#:~:text=The%20Research%20and%20Markets%20report,spraying%20drones.%E2%80%9D%20Moreover,%20the> (accessed on 25 June 2024).
- Jenkins, D.; Vasigh, B. *The Economic Impact of Unmanned Aircraft Systems Integration in the United States*; Association for Unmanned Vehicle Systems International (AUVSI): Arlington, VA, USA, 2013.

4. Goldman Sachs Research. Drones: Reporting for Work. Available online: <https://www.theverge.com/sponsored/goldman-sachs-drones/mobile> (accessed on 25 April 2022).
5. Australian Pesticides and Veterinary Medicines Authority (APVMA). *State of the Knowledge Literature Review on Unmanned Aerial Spray Systems in Agriculture*; Australian Government: Canberra, Australia, 2021; p. 34.
6. Chen, H.; Lan, Y.; Fritz, B.K.; Hoffmann, W.C.; Liu, S. Review of agricultural spraying technologies for plant protection using unmanned aerial vehicle (UAV). *Inter. J. Agric. Biol. Eng.* **2021**, *14*, 38–49. [[CrossRef](#)]
7. Organisation for Economic Co-operation and Development (OECD). *Report on the State of the Knowledge—Literature Review on Unmanned Aerial Spray Systems in Agriculture*; OECD Publishing: Paris, France, 2021.
8. Chen, P.; Douzals, J.P.; Lan, Y.; Cotteux, E.; Delpuech, X.; Pouxviel, G.; Zhan, Y. Characteristics of unmanned aerial spraying systems and related spray drift: A review. *Front. Plant Sci.* **2022**, *13*, 870956. [[CrossRef](#)] [[PubMed](#)]
9. Wang, G.; Han, Y.; Li, X.; Andaloro, J.; Chen, P.; Hoffmann, W.C.; Han, X.; Chen, S.; Lan, Y. Field evaluation of spray drift and environmental impact using an agricultural unmanned aerial vehicle (UAV) sprayer. *Sci. Total Environ.* **2020**, *737*, 139793. [[CrossRef](#)] [[PubMed](#)]
10. Koo, D.; Goncalves, C.G.; Askew, S.D. Agricultural spray drone deposition, Part 2: Operational height and nozzle influence pattern uniformity, drift, and weed control. *Weed Sci.* **2024**, *72*, 824–832. [[CrossRef](#)]
11. Wongsuk, S.; Zhu, Z.; Zheng, A.; Qi, P.; Li, Y.; Huang, Z.; Han, H.; Wang, C.; He, X. Assessing the potential spray drift of a six-rotor unmanned aerial vehicle sprayer using a test bench and airborne drift collectors under low wind velocities: Impact of atomization characteristics and application parameters. *Pest Manage. Sci.* **2024**, *80*, 6053–6067. [[CrossRef](#)]
12. Teske, M.E.; Bird, S.L.; Esterly, D.M.; Curbisiley, T.B.; Ray, S.L.; Perry, S.G. AgDRIFT: A model for estimating near-field spray drift from arial applications. *Environ. Toxic. Chem.* **2002**, *21*, 659–671. [[CrossRef](#)]
13. Martin, D.E.; Latheef, M.A. Payload Capacities of Remotely Piloted Aerial Application Systems Affect Spray Pattern and Effective Swath. *Drones* **2022**, *6*, 205. [[CrossRef](#)]
14. Fritz, B.K.; Hoffmann, W.C.; Wolf, R.E.; Bretthauer, S.; Bagley, W.E.; Bernards, M.L. Wind Tunnel and Field Evaluation of Drift from Aerial Spray Applications with Multiple Spray Formulations. In *Pesticide Formulation and Delivery Systems: 32nd Volume, Innovating Legacy Products for New Uses*; Devisetty, B., Ed.; ASTM International: West Conshohocken, PA, USA, 2013; Volume 32, pp. 96–113. [[CrossRef](#)]
15. Martin, D.E.; Woladt, W.E.; Latheef, M.A. Effect of Application Height and Ground Speed on Spray Pattern and Droplet Spectra from Remotely Piloted Aerial Application Systems. *Drones* **2019**, *3*, 83. [[CrossRef](#)]
16. Whitney, R.W.; Gardisser, D.R. *DropletScan Operator Manual*; WRK of Oklahoma and WRK of Arkansas: Stillwater, OK, USA; Fort Smith, AR, USA, 2003.
17. ASABE. Spray Nozzle Classification by Droplet Spectra. In *ANSI/ASAE S572.3 (FEB2020)*; ASABE: St. Joseph, MI, USA, 2020.
18. American Society of Agricultural and Biological Engineers (ASABE). *Calibration and Distribution Pattern Testing of Agricultural Aerial Application Equipment*; ASABE: St. Joseph, MI, USA, 2013; Volume ASAE S386.2.
19. Fritz, B.K.; Hoffmann, W.C.; Jank, P. A Fluorescent Tracer Method for Evaluating Spray Transport and Fate of Field and Laboratory Spray Applications. *J. ASTM Inter.* **2011**, *8*, JAI103619. [[CrossRef](#)]
20. Gardisser, D.R. Operation S.A.F.E. for Quality Performance/Web Based Decision Making. Available online: <https://tpsalliance.org/pdf/topics/5A-Gardisser-OperationSAFE-2010.pdf> (accessed on 10 February 2024).
21. Carpenter, T.G.; Reichard, D.L.; Khan, A.S. Spray Deposition from a Row-Crop Airblast Sprayer. *Trans. ASAE* **1983**, *26*, 338–0342. [[CrossRef](#)]
22. Grift, T.E.; Walker, J.T.; Gardisser, D.R. Spread Pattern Analysis Tool (SPAT): II. Examples of Aircraft Pattern Analysis. *Trans. ASAE* **2000**, *43*, 1351–1362. [[CrossRef](#)]
23. Yates, W.E. Spray Pattern Analysis and Evaluation of Deposits from Agricultural Aircraft. *Trans. ASAE* **1962**, *5*, 49–0053. [[CrossRef](#)]
24. Whitney, R.W.; Kuhlman, D.K. Pattern Analysis of Agricultural Aircraft. *SAE Trans.* **1983**, *92*, 169–177. Available online: <https://www.jstor.org/stable/44647596> (accessed on 26 March 2024).
25. Smith, D.B.; Oakley, D.; Williams, E.; Kirkpatrick, A. Broadcast Spray Deposits from Fan Nozzles. *Appl. Eng. Agric.* **2000**, *16*, 109–113. [[CrossRef](#)]
26. Justus, C.G.; Mikhail, A. Height variation of wind speed and wind distributions statistics. *Geophy. Res. Lett.* **1976**, *3*, 261–264. [[CrossRef](#)]
27. Ragheb, M. Wind Shear Roughness Classes and Turbine Energy Production. Available online: <http://www.ragheb.co/NPRE%20475%20Wind%20Power%20Systems/Wind%20Shear%20Roughness%20Classes%20and%20Turbine%20Energy%20Production.pdf> (accessed on 10 June 2021).
28. ASABE. *ASAE Standard S561.1; Procedure for Measuring Drift Deposits from Ground, Orchard, and Aerial Sprayers*; American Society of Agricultural and Biological Engineers (ASABE): St. Joseph, MI, USA, 2005.
29. Kuznetsova, A.; Brockhoff, P.B.; Christensen, R.H.B. lmerTest Package: Tests in Linear Mixed Effects Models. *J. Stat. Softw.* **2017**, *82*, 26. [[CrossRef](#)]

30. R Core Team. *R: A Language and Environment for Statistical Computing*; Version 4.2.0; R Foundation for Statistical Computing: Vienna, Austria, 2022.
31. Jaeger, B. r2glmm: Computes R Squared for Mixed (Multilevel) Models. R Package Version 0.1. 2017. Available online: <https://CRAN.R-project.org/package=r2glmm> (accessed on 20 June 2021).
32. Edwards, L.J.; Muller, K.E.; Wolfinger, R.D.; Qaqish, B.F.; Schabenberger, O. An R2 statistic for fixed effects in the linear mixed model. *Statist. Med.* **2008**, *27*, 6137–6157. [[CrossRef](#)]
33. Wickham, H. *ggplot2: Elegant Graphics for Data Analysis*; Springer: New York, NY, USA, 2016. Available online: <https://ggplot2.tidyverse.org> (accessed on 20 June 2021).
34. SAS Institute Inc. *SAS® Software 9.4*; SAS Institute Inc.: Cary, NC, USA, 2013.
35. SAS Institute Inc. *SAS/JMP®*; Version 16; SAS Institute Inc.: Cary, NC, USA, 2023.
36. Lenth, R. Emmeans: Estimated Marginal Means, Aka Least-Squares Means. R Package Version 1.10.6-090003. 2025. Available online: <https://rvlenth.github.io/emmeans/> (accessed on 20 June 2021).
37. Wang, C.L.; Zeng, A.J.; He, X.K.; Song, J.L.; Herbst, A.; Gao, W. Spray Drift Characteristics Test of Unmanned Aerial Vehicle Spray Unit Under Wind Tunnel Conditions. *Inter. J. Agric. Biol. Eng.* **2020**, *13*, 13–21. [[CrossRef](#)]
38. Teske, M.E.; Wachspress, D.A.; Thistle, H.W. Prediction of Aerial Spray Release from UAVs. *Trans. ASABE* **2018**, *61*, 909–918. [[CrossRef](#)]
39. Hunter, J.E.; Gannon, T.W.; Richardson, R.J.; Yelverton, F.H.; Leon, R.G. Coverage and drift potential associated with nozzle and speed selection for herbicide applications using an unmanned aerial sprayer. *Weed Technol.* **2020**, *34*, 235–240. [[CrossRef](#)]
40. Yang, F.; Xue, X.; Cai, C.; Sun, Z.; Zhou, Q. Numerical Simulation and Analysis on Spray Drift Movement of Multirotor Plant Protection Unmanned Aerial Vehicle. *Energies* **2018**, *11*, 2399. [[CrossRef](#)]

Disclaimer/Publisher’s Note: The statements, opinions and data contained in all publications are solely those of the individual author(s) and contributor(s) and not of MDPI and/or the editor(s). MDPI and/or the editor(s) disclaim responsibility for any injury to people or property resulting from any ideas, methods, instructions or products referred to in the content.